Anal. Chem. **1999,** *71,* 4669−4678

Microfabricated Centrifugal Microfluidic Systems: Characterization and Multiple Enzymatic Assays

David C. Duffy,* Heather L. Gillis, Joe Lin, Norman F. Sheppard, Jr., and Gregory J. Kellogg*

Gamera Bioscience, 200 Boston Avenue, Medford, Massachusetts 02155

This paper describes a microfluidic system in which fluids are pumped by centrifugal force through microscopic channels defined in a plastic disk in order to perform complex analytical processes. The channels are created either by casting poly(dimethylsiloxane) against molds fabricated by photolithography or by conventional machining of poly(methyl methyacrylate). The channels have a wide range of diameters (5 μm−0.5 mm) and depths (16 μm−3 mm). Fluids are loaded into reservoirs near the center of the disk, the disk is rotated on the shaft of a simple motor at 60−3000 rpm, and the fluids are pumped outward by centrifugal force through microfluidic networks. The control of flow in the time domain, i.e., gating, is achieved by the use of passive valves based on capillary forces. Flow rates ranging from 5 nL/s to >0.1 mL/s have been achieved using channels of different dimensions and different rates of rotation. The method of pumping is insensitive to many physicochemical properties of the liquid, such as pH and ionic strength, so it has been possible to pump biological fluids, such as blood and urine, a buffer containing a detergent, and some organic solvents. A system that performs multiple (48) enzymatic assays simultaneously using colorimetric detection on a dedicated instrument has been demonstrated. These integrated assays have been used both to yield the Michaelis constant (K_m) of an enzyme and to determine the dose response of an enzyme to a drug. The fluid pumping and control embodied in this system may be readily integrated with other analytical components (e.g., heating, detection, and informatics) to form the basis for a microscale total analysis system for use in genomics, proteomics, high-throughput screening, and molecular diagnostics.

There is currently great interest in combining the functional components that are necessary for performing complex chemical and biochemical analyses into small, integrated units. These integrated units have been described as microscale total analysis systems (μTAS) or laboratories-on-a-chip.[1−4] These systems have the potential to be of great importance in genomics, drug screening, and clinical applications. Microfluidics, i.e., the control of flow of small volumes (from fL to mL) of liquids in microscopic (1−1000 μm) channels, is the central technology in this field. Microfluidic systems[5,6] require the design, fabrication, and implementation of the appropriate pumps, valves, and mixing elements needed to carry out generic manipulations of fluids. In this paper, we describe a microfluidic system based on centrifugal force that complements many of the systems that have been reported previously.

Several methods for controlling the flow of liquids in microfluidic systems have been reported,[5] and electrokinetic control in microfabricated capillaries has received the most attention.[7] Electrokinetic control has several features that make it an attractive option for miniaturized systems: (i) pumping of fluids in the channels, which arises from electroosmotic flow (EOF) in capillaries with charged walls, and the control of the direction of flow are easy to implement and require only a computer-controlled high-voltage (1−30 kV) power supply, electrodes, and a series of relays; (ii) in electrophoretic mode, electrokinetic control results in separations of molecules by size and charge and can be used for chemical analysis; (iii) the microscopic (<100 μm) channels required to generate EOF can be defined in a number of materials, e.g., glass, quartz, and polymers, using microfabrication. Electrokinetic pumping has some disadvantages as a method of controlling the flow of fluids, however. First, it is sensitive to the physicochemical properties, such as ionic strength and pH, of the fluid being pumped. For example, liquids with high ionic strength cannot be pumped using EOF due to excessive Joule heating;[8] it is, therefore, difficult or impossible to pump biological fluids, such as blood and urine, by this method. Second, the high-voltage power supplies used have adverse safety implications and power and space requirements. Third, because electrokinetic pumping requires continuity in the fluid in the channels, it does not work in the presence of trapped bubbles (e.g., air), and care has to be taken to ensure that the channels are free of bubbles. Finally, and most importantly, although EOF is well suited to controlling

* Corresponding authors: (e-mail) dduffy@gamerabioscience.com and gkellogg@gamerabioscience.com; (tel) (781) 306 0827; (fax) (781) 306 0837.

(1) Harrison, D. J., van den Berg, A., Eds. *Micro Total Analysis Systems '98*; Kluwer Academic Publishers: Dordrecht, 1998.

(2) Manz, A., Becker, H., Eds. *Microsystem Technology in Chemistry and Life Sciences*; Springer-Verlag: Berlin, Germany, 1998.

(3) Ramsey, J. M.; Jacobsen, S. C.; Knapp, M. R. *Nature Med.* **1995**, *1*, 1093−1096.

(4) Kricka, L. J.; Wilding, P. Micromechanics and Nanotechnology. In *Handbook of Clinical Automation, Robotics, and Optimization*; Kost, G. J., Welsh, J., Eds; John Wiley and Sons: New York, 1996: pp 45−77.

(5) Kovacs, G. T. A. *Micromachined Transducers Sourcebook*; WCB/McGraw-Hill: Boston, 1998.

(6) Madou, M. *Fundamentals of Microfabrication*; CRC Press: Boca Raton, FL, 1997; pp 426−447.

(7) For a review, see: Effenhauser, C. S.; Bruin, G. J. M.; Paulus, A. *Electrophoresis* **1997**, *18*, 2203−2213.

(8) Grossman, P. D., Colburn, J. C., Eds. *Capillary Electrophoresis: Theory and Practice*; Academic Press: San Diego, 1992; pp 4−14.

10.1021/ac990682c CCC: $18.00
Published on Web 09/11/1999

small volumes of liquids in narrow (<100 μm) channels, it cannot be used to pump liquids at high flow rates (>1 μL/s) in wider channels—a capability that is needed for some microfluidic applications, e.g., sample preparation—because of Joule heating.

A possible alternative to the established methods of controlling the flow of liquids in microfluidic systems is one based on centrifugal force. A centrifugal pump only requires a simple motor, so it is safe and has lower power and space requirements. Pumping in such a system is relatively insensitive to the chemical properties of the liquid, i.e., it works over a range of ionic strengths and values of pH. A centrifugal pump can work when air as well as liquid is present in the microfluidic network, as the pump works naturally to dispel bubbles of gas. Finally, centrifugal pumping can be implemented in a wide range of channel sizes (5 μm to >1 mm), so has the potential to pump liquids over a wide range of flow rates.

A system based on centrifugal force would, however, have to incorporate the fundamental fluid control capabilities, i.e., the spatial and temporal control over the position of fluids in microscopic channels, that have been refined in electrokinetic systems. Here, we report a microfluidic system based around a centrifugal pump that addresses these needs. In our system, a circular plastic substrate or disk containing sealed microfluidic channels is rotated, and the resulting centrifugal force pumps liquids loaded near the center of the disk toward its edge through the fluidic network. Several systems based on centrifugal force, e.g., the GeMSAEC analyzer,[9] were developed in the 1960s and 1970s. These systems, which were composed of deep (several mm) cuvettes connected by channels with diameters of >1 mm that were injection molded in plastic, performed simple fluidic functions (e.g., mixing of sample and reagent) on large volumes (typically >100 μL) of liquids.[10] Liquids were moved between these cuvettes and mixed by rapid acceleration and deceleration of the rotor. More recently, a rotor analyzer has been reported that performs tests on ~100 μL of blood.[11,12]

Our centrifugal system has several advantages over previous designs. First, we have adopted techniques used in the microfabrication industry to define networks of microscopic channels on planar substrates, and this approach confers several benefits. We have been able to span a wide range of flow rates (5 nL/s to 0.1 mL/s) by fabricating channels with dimensions as small as 5 μm × 16 μm and as large as 340 μm × 500 μm. Microfabrication, and photolithography in particular, have allowed us to increase the complexity and density of the fluidic structures compared to those formed by conventional machining and injection molding. Because light was used to define features with high resolution in our method of fabrication, the effect of the roughness of the walls of channels in the polymeric replicas was minimized and the flow of liquid was reproducible. Second, we have developed a number of active and passive valves that effectively gate the flow of liquid in a centrifugal microfluidic system. Third, we present an integrated system: we have developed components to pump, to gate flow, to filter, to mix, to heat, and to detect analytes.[13] We demonstrate some of these capabilities in this paper and illustrate an integrated system based on a colorimetric enzymatic assay.

In this paper, we first describe the fabrication of the microfluidic devices using conventional machining and a rapid prototyping method that is based on photolithography and molding of a polymer. We present a characterization of centrifugal pumping of aqueous, biological, and organic liquids in these devices and compare the experimental results with theory. The gating of fluid flow using passive, capillary burst valves is then presented. We describe how a combination of centrifugal pumping, passive capillary valves, and colorimetric detection was used to carry out multiple (48) enzymatic assays on a disk. We conclude by comparing our method of fluid control to others used commonly in μTAS.

EXPERIMENTAL SECTION

Fabrication. *Rapid Prototyping.* This method is based on photolithography and casting of poly(dimethylsiloxane) (PDMS); it has been described in detail before.[14] Briefly, molds for the casting of polymeric replicas were prepared by photolithography. A fluidic structure was designed first in a computer-aided design (CAD) software package (AutoCAD, Autodesk Inc., San Rafael, CA, or Freehand 7.0, Macromedia, San Francisco, CA). This design was then converted into a photomask. The photomask was usually a pattern of emulsion printed onto a transparency using an image setter with a resolution of 3386 dpi. These masks could be used to pattern features of photoresist greater than 20 μm in diameter.[14] For smaller features, a pattern of chrome on quartz was used as the photomask. A 125-mm-diameter Si wafer (Silicon Inc., Kuna, IA) was coated in a layer of negative photoresist (SU-8 (50), Microlithography Corp., Newton, MA) using a spin-coater (KW-4A, Chemat Technology Inc., Northridge, CA). After baking, the wafer was exposed to UV light (200-W Hg lamp, 177-mm-diameter lens; Hybralign 400 Mask Aligner, Optical Associates Inc., Milpitas, CA) through the photomask. Details of the processing parameters for the SU-8 photoresist are given elsewhere.[14,15] The resist was then developed in propylene glycol methyl ether acetate (PGMEA; Aldrich, Milwaukee, WI) to reveal a mold composed of a pattern of positive relief photoresist. The thickness of the photoresist, which is equal to the depth of the channels in the polymeric replica, was measured on a profilometer (Sigmascan, Tencor Instruments, Mountain View, CA). The mold was passivated by exposing it to a vapor of tridecafluoro-1,1,2,2-tetrahydrooctyl-1-trichlorosilane (United Chemical Technologies, Bristol, PA) for 2 h. A 10:1 mixture of PDMS oligomer and cross-linking agent (Sylgard 184, Dow Corning, Midland, MI), which had been degassed under vacuum, was poured onto the mold. For colorimetric measurements, we created disks that were reflective to visible light by adding 1 wt % of a white pigment (Createx Liquid Pure Pigment Titanium White, Createx Colors, E. Granby, CT) to the PDMS mixture before degassing the polymer. The polymer was then cured at 65 °C for 1 h before the replica composed of a pattern of negative relief channels was peeled from the mold.

(9) Scott, C. S.; Burtis, C. A. *Anal. Chem.* **1973**, *45*, 327A−340A.
(10) Scott, C. S.; Burtis, C. A. *Centrifugal Analysis in Clinical Chemistry*; Praeger: New York, 1980.
(11) Schembri, C. T.; Ostoich, V.; Lingane, P. J.; Burd, T. L.; Buhl, S. N. *Clin. Chem.* **1992**, *38*, 1665−1670.
(12) Schembri, C. T.; Burd, T. L.; Kopfsill, A. R.; Shea, L. R.; Braynin, B. *J. Autom. Chem.* **1995**, *17*, 99−104.
(13) Madou, M.; Kellogg, G. J. *Proc. SPIE* **1998**, *3259*, 80−93.
(14) Duffy, D. C.; McDonald, J. C.; Schueller, O. J. A.; Whitesides, G. M. *Anal. Chem.* **1998**, *70*, 4974−4984.
(15) Lorenz, H.; Despont, M.; Fahrni, N.; Brugger. J.; Renaud, P.; Vettiger, P. *Sens. Actuators A* **1998**, *64*, 33−39.

Conventional Machining. Designs were created in AutoCAD and uploaded as files to program a milling machine (Benchman VMC-4000, Light Machines Corp., Manchester, NH). The designs were then machined in poly(methyl methacrylate) (PMMA; ICI Acrylics, St. Louis, MO) using end mills ranging in diameter from 125 μm to 1.59 mm. In some cases, the machined parts were replicated in PDMS by casting and curing the prepolymer against the machined part. This negative replica in PDMS was then oxidized in an oxygen plasma (see below) for 1 min and exposed to the fluorinated silane for 2 h to provide a surface with low adhesion to PDMS. Finally, PDMS was cast against the negative replica, cured and peeled away to reveal a positive replica of the machined part.

Sealing of Microfluidic Channels. For most applications, the PDMS replica containing the microfluidic channels was sealed reversibly and conformally to a piece of PMMA that had macroscopic reservoirs (typical volumes of up to 100 μL) machined into it. In some cases, the PDMS replica (contact angle of water, $\theta \sim 90°$) was rendered hydrophilic ($\theta \sim 50°$) by leaving it in 9% HCl for 2 h. The PMMA layer and PDMS replica were aligned so that liquid could be pumped from the reservoirs into the microfluidic channels. In this system, the reversible seal allowed the two layers of the disk to be peeled apart, cleaned, resealed, and reused. For precise measurements of burst frequencies of the capillary valves, we fabricated devices in which all four walls of the channels were made from the same material by sealing the PDMS replicas against a PDMS replica of a machined part that contained reservoirs. For applications in which it was desirable to eliminate the chance of leakage of liquids from the channels and reservoirs, e.g., for the pumping of blood, the two PDMS layers were sealed tightly and irreversibly using a method that has been described previously.[14] Briefly, the two pieces of PDMS were placed in a plasma etcher (Plasma System 500-II, Technics Inc., Pleasanton, CA) and oxidized for 1 min. Immediately after the plasma treatment, the two pieces were aligned and brought into conformal contact to form a tight seal. Finally, parts machined in PMMA that contained channels as well as reservoirs were sealed against flat pieces of PDMS.

Centrifugal Pumping. Liquids were pumped through the channels by spinning the disks on a hub driven by a dc servomotor with an integral optical encoder (DC MicroMotor 3042/HEDS-5540I, Micro Mo, Clearwater, FL). The servomotor was operated via a motor controller card (PIC-Servo, HdB Electronics, Redwood City, CA) and host PC using a program written in Visual Basic (Microsoft, Redmond, WA). The speed of the motor could be programmed to give rates of rotation of between 0 and 3000 rpm. The encoder triggered external devices such as a tachometer, stroboscope, and frame buffer.

Characterization of Flow. The flow of liquid on the disks was monitored using stroboscopic video microscopy. A fast response stroboscope (NovaStrobe DA116, Monarch Instruments, Amherst, NH) was triggered by the encoder and illuminated the spinning disk for 30 μs, once per revolution. An image of the spinning disk was continually recorded by a $^1/_3$-in. CCD color video camera (GP-KR222, Panasonic, Tokyo, Japan) with macrofocus zoom lens. The rate of rotation recorded by the tachometer (08212, Cole-Parmer, Vernon Hills, IL) was displayed simultaneously using a digital video mixer. To give a continuous illuminated image of the disk, dark frames were filtered out using a frame buffer (Ultra II, Coreco, Saint-Laurent, Quebec, Canada).

Flow rates were determined by measuring the time required for a liquid to fill a sealed chamber of known volume. Small amounts (<1% vol) of food coloring were added to deionized water to assist the visualization of aqueous solutions. Measurements of the flow rates of blood were carried out on fresh bovine samples. The fraction of the blood that was composed of red blood cells, i.e., the hematocrit, was varied by centrifuging the blood and mixing appropriate volumes of plasma and red blood cells.

Capillary Burst Valves. A PDMS replica containing 20 capillaries ranging in diameter from 20 to 500 μm was fabricated by rapid prototyping. This replica was sealed to a layer of PDMS containing reservoirs for liquids. The burst frequencies of each of the capillaries was observed using video microscopy as the rate of rotation of the disk was increased at 10 rpm/s.

Multiple Enzymatic Assays. A fluidic structure that allowed mixing of an enzyme and inhibitor, followed by mixing with a substrate, and detection of the product, was designed in CAD (Figure 1A). This structure was repeated 48 times on the disk (Figure 1B). A mold and PDMS replicas of this design were created by rapid prototyping, and the replicas were sealed against machined reservoir layers (Figure 1C). Solutions of alkaline phosphatase (EC 3.1.3.1, from human placenta, Sigma, St. Louis, MO), theophylline (Sigma), and *p*-nitrophenol phosphate (PNPP; Sigma) were made up in buffer (0.1 M glycine, 0.5 mM $MgCl_2$ in deionized water). Aliquots (3 μL) of enzyme, 3-μL aliquots of theophylline (inhibitor), and 6-μL aliquots of PNPP (substrate) were then loaded into the respective 48 reservoirs using a micropipet. The disk was then run on a centrifugal colorimetric instrument. This instrument was similar in design to the video microscopy apparatus, except that instead of a video camera, a standard spectrophotometric detector head,[16] which was composed of an array of three light emitting diodes (LED; 430, 660, 590 nm) and two photodiode detectors, allowed measurements of reflectance at three visible wavelengths of cuvettes on the outer edge of the disk.[16]

The sequence of operations performed in each assay was as follows. First, after loading each solution of enzyme, inhibitor, and substrate into reservoirs labeled in parts A−C of Figure 1 as R1, R2, and R3, respectively, the solutions of enzyme and inhibitor were pumped to capillary valves V1. Increasing the rate of rotation caused both solutions to burst through the valves at the same time: this process maximized mixing of the two solutions. The combined solutions were then pumped through a meandering 100-μm-wide channel (C1) in which they mixed by diffusion. At the same time, the solution of substrate was pumped through another channel (C2). The mixture of enzyme and inhibitor and the solution of substrate then met at another pair of capillary valves (V2). A further increase in the rate of rotation caused the solutions to burst through these valves into a chamber. These solutions were then pumped through another meandering channel (C3) where mixing by diffusion allowed the enzyme and substrate to react. The lengths of all the channels and the size of the reservoirs were chosen to give flow rates such that the reactions between the enzyme, substrate, and inhibitor were stoichiometric and that

(16) Norman, R. A. *Principles of Bioinstrumentation*; Wiley: New York, 1988; pp 283−308.

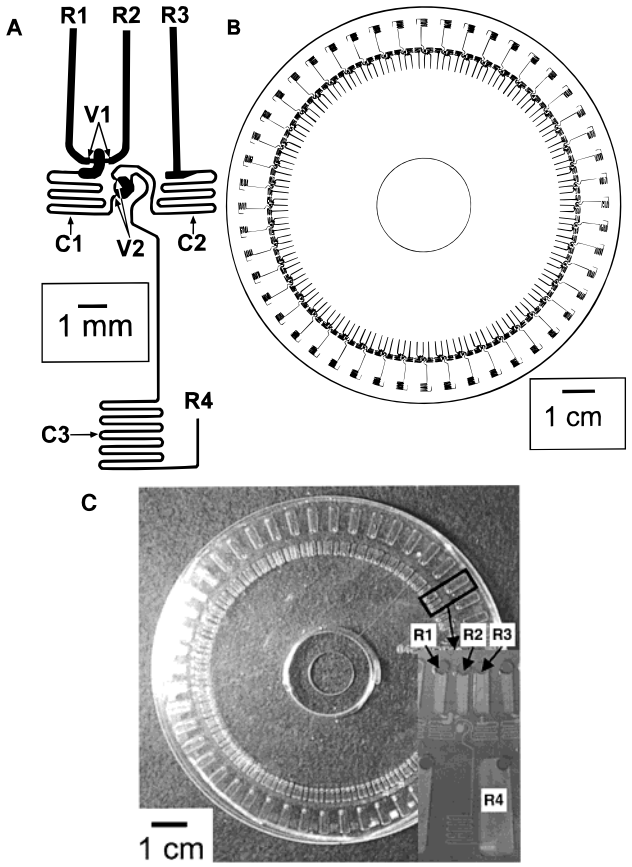

Figure 1. (A) Design of the fluidic structure used to perform an assay composed of mixing an enzyme with an inhibitor, followed by mixing with a substrate, and detection. The solutions of enzyme, inhibitor, and substrate were loaded in reservoirs that were connected to channels labeled R1, R2, and R3, respectively. Enzyme and inhibitor combined after being released by capillary burst valves, V1, and mixed in a meandering 100-μm-wide channel, C1. The enzyme−inhibitor mixture was combined with the substrate in a chamber after being released by capillary valves, V2. These solutions mixed in a meandering channel, C3, and emptied into a cuvette (not shown) from a section of channel labeled R4. (B) Design for the photomask used to create PDMS replicas for carrying out 48 enzymatic assays simultaneously. The design was created by rotating the fluidic structure shown in (A) about the center of a 120-mm-diameter circle by 7.5° 48 times. (C) Photograph of the disk composed of a PDMS replica that was fabricated by rapid prototyping using a photomask generated from the design in (B) and sealed to a layer of PMMA with reservoir layers machined into it. The inset shows a magnified detail of one of the fluidic structures of the disk. The labels indicate the various reservoirs in the PMMA layer.

mixing could be achieved by diffusion.[17] For each of the 48 structures, this reaction solution then filled a cuvette (R4). The disk was then slowed and the three LEDs were pulsed in sequence to measure the intensity of light at each wavelength reflected from each of the 48 cuvettes. These intensities were converted to reflectances by normalizing to the intensity of a fraction of the incident light that was split off and measured by a reference photodiode. The values of reflectance (I/I_o) were then used to calculate absorbance ($A = -\log(I/I_o)$). As the product of the enzyme−substrate reaction, *p*-nitrophenol, has a peak in absorption at 410 nm, its concentration was approximately proportional to $A_{430\ nm} - A_{660\ nm}$, where $A_{430\ nm}$ was the absorbance at 430 nm and $A_{660\ nm}$ the absorbance at 660 nm. The whole process—from spin profile to detection and acquisition—was controlled by a host PC and software.

RESULTS AND DISCUSSION

Fabrication. Devices were fabricated either by conventional machining[18] or by a microfabrication methodology (rapid prototyping).[14] Designs for fluidic networks were created by CAD, and the whole design and fabrication process could be carried out in less than 24 h for both methods of fabrication. A typical design of a fluidic network is shown in Figure 1.

Conventional machining was used to create channels and chambers in PMMA with depths ranging from 125 μm to 3 mm and widths of >125 μm. Machining can also provide parts containing channels and reservoirs with different depths. To create narrower (down to 5 μm wide) and shallower (down to 16 μm deep) channels, we cast PDMS against molds of positive relief photoresist prepared using photolithography.[14] We have also used this method to produce larger structures with dimensions similar to those produced by conventional machining. For example, we used rapid prototyping to prepare replicas containing channels with depths up to 350 μm and widths up to 1 mm. Although rapid prototyping could, in principle, be used to create replicas containing channels of more than one thickness by fabricating molds with multiple layers of photoresist,[19] we chose to fabricate disks composed of two halves that have features with different depths defined on them. In particular, our disks were usually composed of a PDMS replica that contained small (<100 μm) channels sealed to a piece of PMMA (or a PDMS replica of it) that had deep (typically 300−900 μm) reservoirs machined in it (Figure 1C).

Pumping by Centrifugal Force. We characterized experimentally the flow rate of aqueous solutions pumped by centrifugal force in channels that had a wide range of diameters and compared the results to simple centrifuge theory. For a liquid flowing through a channel from a reservoir (Figure 2), the average velocity of the liquid (U) and its volumetric flow rate (Q) depend on the rheological properties of the liquid, the size, location, and configuration of the channels, and the rate of rotation, through eqs 1 and 2, where ρ and η are the density and viscosity of the

$$U = d_H^2 \rho \omega^2 \bar{r} \Delta r / 32 \eta L \quad (1)$$

$$Q = UA = A d_H^2 \rho \omega^2 \bar{r} \Delta r / 32 \eta L \quad (2)$$

liquid, respectively, A is the cross-sectional area of the channel, d_H is the hydraulic diameter of the channel (defined as $4A/P$, where P is the perimeter of the channel), L is the length of the channel, ω is the angular velocity, $\bar{r}$ is the average distance of the liquid in the channels from the center of the disk, and Δr is the radial extent of the fluid subject to centrifugal force. We find it convenient to define $\bar{r}$ and Δr in terms of r_0, r_1, and H, the head of the liquid in the reservoir that feeds the channel, such that, $\bar{r} = (r_1 + (r_0 - H))/2$ and $\Delta r = r_1 - (r_0 - H)$. The geometric parameters are shown schematically in Figure 2.

(17) Galambos, P.; Forster, F. K. in ref 1, pp 189−192.

(18) Walker, J. R. *Machining Fundamentals*; Goodheart-Willcox Co.: South Holland, IL, 1993.

(19) Renaud, P.; van Lintel, H.; Heuschkel, M.; Guérin, L. in ref 1, pp 17−22.

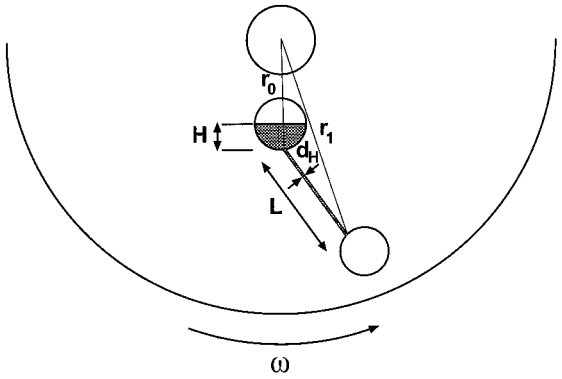

Figure 2. Schematic diagram of a liquid being pumped through a simple fluidic network in a centrifugal system. The disk contains two reservoirs connected by a channel. The critical parameters that determine the flow rate of liquids being pumped by centrifugal force in this network are labeled. r_0 and r_1 are the inner and outer radii of the flowing fluid, respectively; H is the "head" of liquid in the feed reservoir; d_H is the hydraulic diameter of the channel; L is the length of the channel; ω is the rate of rotation of the spinning disk.

Equation 1 assumes that the flow in the channels is laminar, i.e., nonturbulent. We verified this assumption by calculating the Reynolds numbers (*Re*) of flow in these channels and comparing them to values for turbulent flow observed in other systems. *Re* is given by the ratio of the inertial forces to the viscous forces in the flow of liquid:

$$Re = \rho U l / \eta \qquad (3)$$

where l is the characteristic length scale of the device, usually taken as equal to d_H.[5] Based on observation of the velocities of liquids in the largest channels we have used, *Re* has a maximum value on the order of 100 and is usually much lower in the microscopic channels used here. These Reynolds numbers are lower than those at which turbulence occurs ($Re > 2300$),[5] so it is reasonable to assume that eq 1 describes accurately the velocity of liquids in these systems.

Figure 3 shows the experimental flow rates plotted against the theoretical flow rates calculated using eq 2. Several parameters were varied in these experiments. Data were obtained at different rates of rotation (from 400 to 1600 rpm) for a number of microfabricated devices that contained channels with different widths (20−500 μm), depths (16−340 μm), and lengths (12.5−182 mm). Data are also included for devices created by conventional machining followed by replication in PDMS. In some experiments, the viscosity of the fluid was increased by a factor of 10 by adding 20 wt % poly(ethylene glycol) to water.

The coefficient of variation of the experimental flow rates from the theoretical flow rates in microfabricated channels was 18.5%. Experimental errors in the measurement of the highest and lowest flow rates made a large (~5−10%) contribution to this coefficient of variation. As Figure 3 shows no systematic deviation of experiment from theory, we conclude that eq 2 adequately describes the flow of aqueous solutions under centrifugal pumping in channels whose dimensions ranged from 20 μm to 0.5 mm. Figure 3 also demonstrates that we have been able to span a wide range of flow rates (5 nL/s to 0.1 mL/s) using centrifugal force. Higher flow rates could be achieved with higher rates of rotation

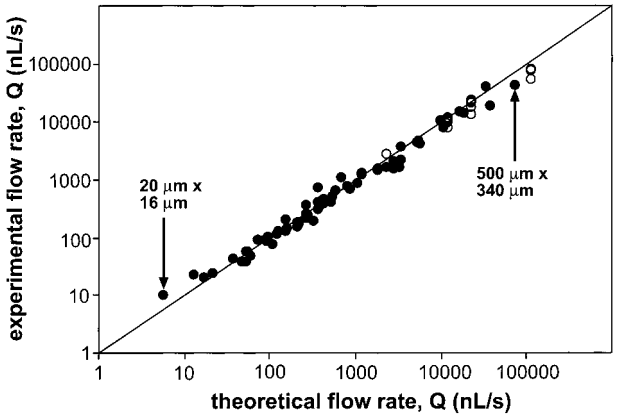

Figure 3. Comparison of the experimental flow rates and the flow rates calculated from a theoretical expression of liquid being pumped in microfluidic channels by centrifugal force (eq 2). The open circles represent data taken with channels in PDMS that were fabricated by replicating a part that had been machined in PMMA. The filled circles represent data taken with channels in PDMS that were fabricated by rapid prototyping. The straight line is the line for which experiment and theory are equal. The data were taken for a range of hydraulic diameters (d_H), channel lengths (L), amounts of liquid in the channels ($\bar{r}$ and Δr), rates of rotation, and viscosities. For example, the replicas of machined masters (open circles) had channels with widths of 250 and 500 μm, and the data were recorded with both aqueous solutions and mixtures of water and poly(ethylene glycol) that had 10 times the viscosity of water. The data from microfabricated devices (closed circles) were obtained from PDMS replicas of six molds that contained 20 channels ranging in diameter from 20 μm to 0.5 mm and had depths ranging from 16 to 340 μm. The largest and smallest microfabricated channels used are indicated on the figure. The rates of rotation ranged from 400 to 1600 rpm.

using motors that can apply greater torques. The range of flow rates we have achieved with centrifugally induced pressure compares favorably to those achieved by other methods of pumping.[5] For examples, EOF in microscopic channels can be used to generate flow rates of typically between 10 nL/s and 0.1 μL/s,[20] micromachined diaphragm or membrane pumps can generate flow rates from 10 nL/s up to 10 μL/s,[5] and electrohydrodynamic pumps can achieve flow rates up to 0.1 mL/s.[5] A single pumping mechanism that can achieve a wide range of flow rates provides a way to address the different requirements between, and within, applications. For example, the pretreatment of crude samples (e.g., filtering of blood) for subsequent clinical and biochemical analysis typically involves volumes of 10−100 μL and will require appropriately large flow rates (>1 μL/s). Other applications, for example, high-throughput screening of drug libraries, require that smaller volumes (<1 μL) be processed and smaller flow rates (~10 nL/s) be achieved.

The good agreement between experiment and theory suggests that the flow of liquids in these channels was laminar in all cases. For the flow of water in the largest microfabricated channel (500 × 340 μm), $Re = 84$, and for the smallest channel (20 × 16 μm), $Re = 0.15$, well below the transition from laminar flow to turbulent flow.[5] The implication of this observation for carrying out chemical reactions in these channels is that mixing will have to be carried out by diffusion,[3] perhaps in specially designed configurations of channels; mixing by turbulence is not an option in these channels.

(20) Paul, P. H.; Arnold, D. W.; Rakestraw, D. J., in ref 1, pp 49−52.

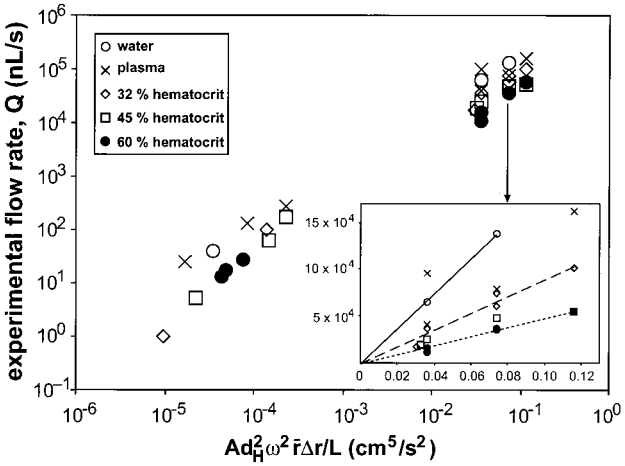

Figure 4. (A) Plot of the flow rates of water, plasma, and whole blood at three values of hematocrit (32, 45, and 60% red blood cells) against a parameter, $Ad_H^2\omega^2\bar{r}\Delta r/L$, that accounts for all of the known variables in these experiments. The data at low flow rates (<1000 nL/s) were obtained using channels with depths of 22 μm and widths ranging from 20 μm to 0.5 mm. The data at high flow rates (>10^4 nL/s) were obtained using channels with widths of 250 and 500 μm and depths of 500 μm. The inset shows detail of the higher flow rates. Linear fits to the data are shown: the solid line is a fit to the water data, the dashed line to the data at 32% hematocrit, and the dotted line to the data at 60%.

Pumping of Biological and Chemical Fluids. One of the main advantages of using centrifugal force is that fluids with different physicochemical properties can be pumped in the microfluidic channels. Centrifugal pumping is relatively insensitive to the physicochemical properties of the liquid such as ionic strength, pH, conductivity, and the presence of analytes that adsorb to the walls of the channels. We have demonstrated this capability by pumping blood, other biological fluids, and an organic solvent.

Figure 4 shows plots of the flow rates under centrifugal pumping of water, plasma, and bovine blood at three values of hematocrit. These measurements were made at a number of different rates of rotation and with channels of different cross sections and lengths. Because blood is a non-Newtonian fluid, we would expect its viscosity to change nonlinearly with flow rate. We have, therefore, plotted the experimental flow rates as a function of a parameter ($Ad_H^2\omega^2\bar{r}\Delta r/L$) that incorporates all of the known experimental variables.

The rheological properties of blood in microscopic channels are well studied,[21,22] and the data shown in Figure 4 illustrate several of the observations that have been made previously. First, the inset to Figure 4 shows that flow rate decreased as hematocrit, i.e., the fraction of red blood cells of the blood samples, was increased. Red blood cells largely determine the rheological properties of blood, and the formation of aggregates of them results in resistance to flow and, hence, an increase in viscosity and a decrease in flow rate as a function of hematocrit. Second, the kinematic viscosities (η/ρ), which can be calculated from the experimental flow rates and eq 2, varied nonlinearly with the average shear rate ($\dot{\gamma} = 4U/d_H$)[23] for whole blood, which is a non-Newtonian fluid, but were independent of $\dot{\gamma}$ for water and plasma, which are Newtonian fluids.[23] Furthermore, the kinematic viscosity of whole blood became increasingly nonlinear with shear rate as the hematocrit was increased from 32 to 60%. The increase in viscosity at lower shear rates at a given hematocrit, and the greater nonlinearity at higher hematocrit, are attributed to shear-dependent changes in the aggregation of red blood cells.[21]

One concern when whole blood is pumped in microscopic channels is the possibility of cells blocking the channels. Some workers have found that channels with a diameter of <50 μm become blocked by whole blood.[22] Similarly, although we could reliably analyze blood samples using channels with diameters of >50 μm, the results with channels with diameters of <50 μm were less reproducible. If the sample of blood was more than a few days old, or if insufficient anticoagulation agent (heparin) had been added to the blood, then these channels had a greater tendency to become blocked.

We have pumped several fluids, other than blood, that are of biological and chemical interest and that provide a challenge for microfluidic pumps. We measured the flow rates (from 20 nL/s to 6 μL/s) of urine, an organic solvent (dimethyl sulfoxide (DMSO)), and a biological buffer that is used in the polymerase chain reaction (PCR), in microfabricated channels that ranged in diameter from 25 to 100 μm. There was good agreement between experiment and theory for all of the liquids.[24] The ability to pump urine shows that this system can handle a liquid with high ionic strength. The ability to pump DMSO suggests that this system could be used for organic chemical synthesis. Such an application would, of course, be dependent on the compatibility of the particular solvent with the polymer. The results with the PCR buffer show that we were also able to pump a solution containing a surfactant (0.1% Triton X-100) near its critical micelle concentration (cmc).

Gating of the Flow of Liquids in Centrifugal Microfluidic Devices. For this system to be useful, the flow of liquid must be controlled in the time domain. We have gated the flow of liquid in these microfluidic networks using a number of passive and active valves. These valves include the following: single-use (initially closed) valves that are actuated by a heat-activated phase change of a solid; single-use (initially open) valves that are actuated by manipulating air pressure; and reusable (normally closed) diaphragm valves that are based on the reversible seal between PDMS and a flat substrate. Here, we describe and characterize the valve that we have used most extensively: a passive, single-use valve that relies on capillary forces and is actuated by centrifugal pressure. This valve was used to gate the flow of liquids in the assays described in the next section.

The operation of this valve is shown schematically in Figure 5. At a low rate of rotation, as liquid flows through a channel and meets an exit into a chamber, it is pinned at the discontinuity in the fluidic network (Figure 5A). For the liquid to exit the channel, sufficient work has to be done by the centrifugal pump to overcome the energetic penalty of forcing the pinned liquid into

(21) Chien, S.; Usami, S.; Skalak, R. In *Handbook of Physiology*; Renkin, E. M., Michel, C. C., Eds.; American Physiological Society: Bethesda, MD, 1984.
(22) Wilding, P.; Pfahler, J.; Bau, H. H.; Zemel, J. N.; Kricka, L. J. *Clin. Chem.* **1994**, *40*, 43−47.
(23) Fung, Y. C. *Biomechanics*, 2nd ed., Springer-Verlag: New York, 1993; pp 66−108.
(24) The flow rates of DMSO were calculated using values of the viscosity and density taken from: *CRC Handbook of Chemistry and Physics*, 78th ed.; Lide, D. R., Ed; CRC Press: Boca Raton, FL, 1997.

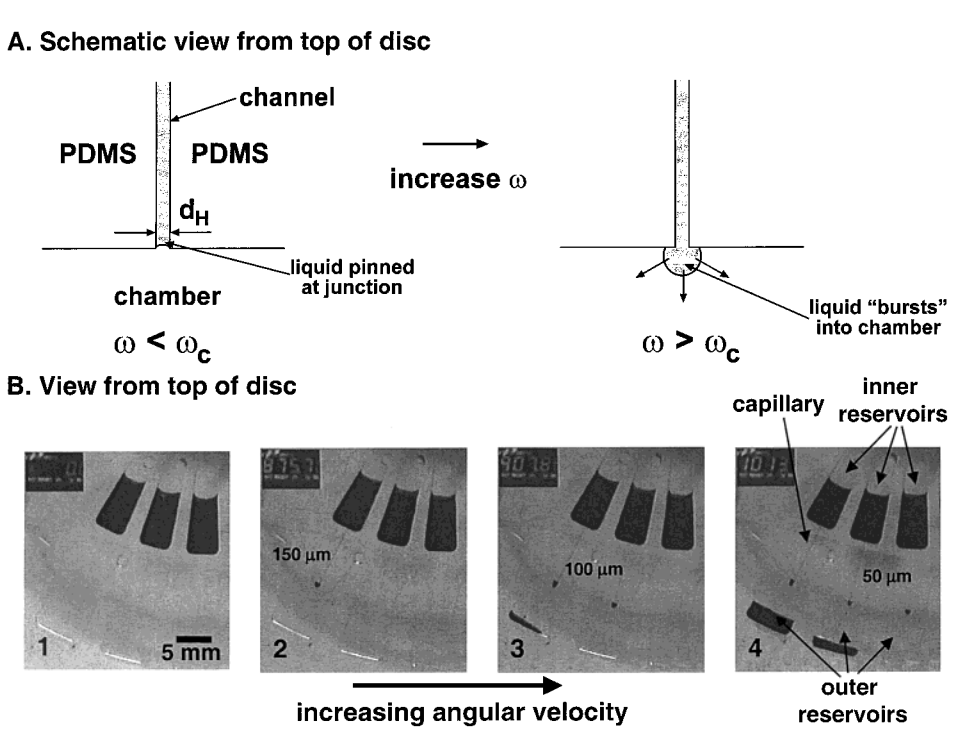

Figure 5. Capillary burst valves. (A) A schematic view from above the disk of a passive capillary burst valve. A liquid flows in a channel or capillary and is pinned at the discontinuity where the channel meets a chamber or a wider channel. Sufficient fluidic pressure must be exerted by the centrifugal pump to overcome the pressure of curved liquid surfaces and to wet the walls of the chamber with liquid. This pressure is achieved at a characteristic rate of rotation or "burst" frequency, ω_c, above which the liquid exits the channel and enters the chamber. ω_c depends on the hydraulic diameter (d_H) of the capillary and the amount of liquid in the channel (see text) and therefore provides a means of gating the flow of liquid. (B) Video stills of a rotating disk containing three capillary burst valves. The number in the top left corner of each image is the rate of rotation in rpm from the tachometer. In this experiment, two reservoirs containing solutions of dye were connected by channels with diameters of 150, 100, and 50 μm, from left to right, respectively. Initially, the disk was stationary (1). The disk was then spun at an acceleration of 10 rpm/s. The capillary valves burst in sequence, with the widest channel bursting at the lowest rate of rotation (2), then the 100-μm-wide channel (3), and finally, the narrowest channel (4).

the chamber. Because the work done by a centrifugal pump increases with the rate of rotation, the liquid exits the channel when the spinning disk reaches a characteristic rate of rotation or "burst" frequency, ω_c, at which the work done by the pump exceeds this energetic penalty (Figure 5A). We therefore call these fluidic control elements capillary burst valves.

An exact solution to determine the burst frequency of a capillary valve that incorporates factors such as surface roughness and the specific geometries of the channels and chambers would be complex. We have, therefore, chosen to adopt a simple model based on capillary forces and empirical measurements of burst frequencies in order to use these structures as valves. By balancing the pressure at the exit of the capillary induced by centrifugal force ($\rho\omega_c^2\bar{r}\Delta r$) with the pressure inside the bubble being formed at the exit of the capillary (given by the Laplace equation)[25] and the pressure required to wet the walls of the chamber, we produce a simple expression (eq 4) that relates ω_c

$$\rho\omega_c^2\bar{r}\Delta r = a(4\gamma/d_H) + b \qquad (4)$$

to the hydraulic diameter of the channel and the position of the liquid on the disk, where γ is the surface tension of the liquid and a and b are empirical constants that are determined by the shape of the droplet, the geometry of the chamber, and the wettability of the walls of the chamber.

From eq 4, it is clear that by taking into account the position of the liquid on the disk and by appropriate adjustment of the diameter of the channels, we can design structures that will release fluids at well-defined rotational rates to provide frequency-dependent valves. For example, Figure 5B shows video stills of a rotating disk that contained a series of three valves composed of capillaries of different widths. The valves with wider capillaries burst at lower frequencies and the narrower capillaries burst at higher frequencies, as expected from eq 4. Several capillary burst valves can be used sequentially in one fluidic network to allow complicated processes.

Figure 6 shows experimental values of $\rho\omega_c^2\bar{r}\Delta r$, i.e., the induced pressure at which a burst was observed, plotted as a function of $1/d_H$ for microfabricated devices with channels ranging in diameter from 20 to 500 μm. According to eq 4, these plots should be linear. The coefficient of variation of the experimental burst frequencies determined from linear fits to these data was 4.3%. We have used the precision of these passive valves to control the flow of liquid in our fluidic networks.

We believe that the precision in gating afforded by these valves is determined by the quality of the microfluidic channels. For example, the burst frequencies of shallower (16 μm) channels had greater coefficients of variation (~10%) than the data for the deeper (167 μm) channels shown in Figure 6. The photoresist

(25) Adamson, A. W.; Gast, A. P. *Physical Chemistry of Surfaces*, 6th ed.; Wiley: New York, 1997; pp 4−8.

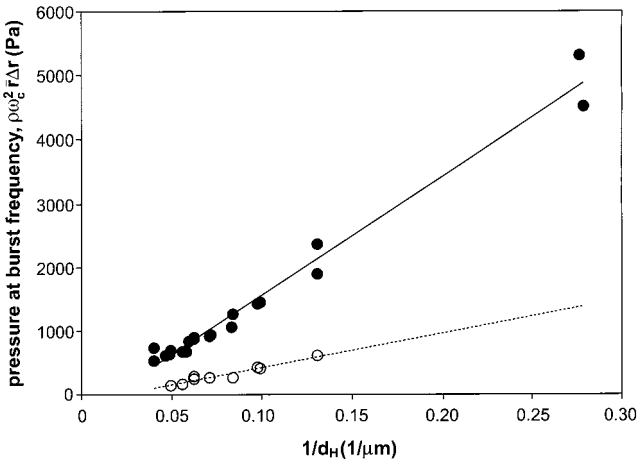

Figure 6. Plots of the pressure exerted by the centrifugal pump ($\rho\omega_c^2\bar{r}\Delta r$) against $1/d_H$ of capillary burst valves. ω_c is the experimental burst frequency of aqueous solutions in channels with hydraulic diameters, d_H. In these experiments, the channels were 167 μm deep and ranged in diameter from 20 to 375 μm. The burst frequencies ranged from 100 to 600 rpm. The filled circles represent data from experiments using water and channels with walls composed of PDMS; the solid line is a straight line fit to these data. The open circles represent data from experiments using the same channels and a PCR buffer that contained 0.1% Triton X-100 surfactant. This solution had a low surface tension (γ < 30 dyn/cm). The dotted line is a straight line fit to these data. The coefficient of variation of the straight line fits (eq 4) from the experimental burst frequencies was 4.3%.

we used to produced the mold for these valves is optimized for thicknesses greater than 50 μm. We would expect, therefore, that variations in the thickness of the 16-μm-thick channels were greater than for the 167-μm-thick channels: such variations would explain the greater variation in burst frequencies.[26] Furthermore, the burst frequencies of valves fabricated by conventional machining,[13] while also following the relationship given in eq 4, had coefficients of variation greater than those in Figure 6. We believe that the greater surface roughness of the channels produced by machining compared to those defined by photolithography leads to this larger error.

One potential limitation of these valves is that liquids with low surface tension, e.g., solutions containing surfactants, tend to wet the walls of the chamber when they reach the end of the capillary and do not get pinned. This effect might limit the use of these valves with liquids of low surface tension. For channels with diameters of >100 μm, we found that the use of these valves with solutions of surfactant (surface tension, $\gamma \approx 20-30$ dyn/cm) was irreproducible because the solution tended to flow out of the capillary into the chambers without pinning. Channels with diameters of <100 μm could, however, be used reliably to gate the flow of solutions of surfactants. For example, Figure 6 shows data for the burst frequencies of capillary valves using a solution containing a surfactant (0.1% Triton X-100), 20 mM Tris-HCl, and 10 mM $MgSO_4$. We note that the ratio of the slopes of the plots in Figure 6 for water and surfactant solutions (3.4) is close to the value we would expect from eq 4 and the relative surface tensions of water ($\gamma = 73$ dyn/cm) and the solution of surfactant ($\gamma = 30$ dyn/cm for Triton X-100 above its cmc; this value will presumably be lower in the presence of Tris and salt).

Multiple Enzymatic Assays. In this section, we describe how we have combined centrifugal pumping in microscopic channels, capillary burst valves, and colorimetric detection to carry out multiple (48) homogeneous enzymatic assays simultaneously. Enzymatic assays are important in clinical diagnostics as well as being of fundamental scientific interest in the investigation of enzymes. The ability to do a large number of enzymatic assays simultaneously is useful for high-throughput screening in diagnostics and the screening of drug libraries.[27] There have been previous reports of assays, both enzymatic[28,29] and immunological,[30−32] in miniaturized systems; these reports focused on single assays.

We chose a model enzyme + inhibitor + substrate system for our multiple assay disks. The enzymatic reaction we selected was dephosphorylation by alkaline phosphatase. The substrate for this reaction was *p*-nitrophenol phosphate: the starting material is colorless and is converted to *p*-nitrophenol, which is yellow and absorbs at 410 nm, by alkaline phosphatase. We monitored the turnover of the enzymatic reaction by measuring the absorption of light at 430 nm by the product. The detection limit of our colorimetric detector for the product of this particular enzyme−substrate reaction was 10 μM in a volume of 12 μL; using a fluorescent substrate and fluorescence detection we have detected 5 nM of substrate in the same volume.[33] The presence of theophylline in solution reduces the rate of reaction between alkaline phosphatase and its substrate, so we used this molecule, which is used as a bronchodilator by asthmatics, as the inhibitor.[34,35]

The design of the fluidic network used for the assay is shown in Figure 1A; this structure was repeated 48 times around the edge of the disk so that 48 assays could be run simultaneously with the same sequence of rates of rotation. A sequence was run so that the following fluidic operations were performed in each structure. The solutions of enzyme and inhibitor were mixed first. Then, this enzyme−inhibitor mixture was combined with a solution of the substrate. The lengths of the channels and the size of the reservoirs were designed so that flow rates of, first, the solutions of the enzyme and inhibitor, and, second, the substrate and enzyme−inhibitor mixture, were the same to get stoichiometric reactions by diffusional mixing. The rates of rotation (and hence the flow rates) were set such that the solutions were in the mixing channels for ~2 s. A calculation of the concentration

(26) We do not believe, however, that the use of these burst valves is limited to thicker channels: by using a photoresist that was optimized for thinner (10 μm) features, reproducible thicknesses and hence burst frequencies could be achieved.

(27) For an example of high-throughput screening of inhibitors using enzymatic assays, see: Ambrose, W. P.; Semin, D. J.; Robbins, D. L.; Van Orden; Kashem; M. A.; Hamilton, S. A.; Nelson, R. M.; Jett, J. H.; Keller, R. A. *Anal. Biochem.* **1998**, *263*, 150−157.

(28) Hadd, A. G.; Raymond, D. E.; Halliwell, J. W.; Jacobsen, S. C.; Ramsey, J. M. *Anal. Chem.* **1997**, *69*, 3407−3412.

(29) Moser, I.; Jobst, G.; Svasek, P.; Varahram, M.; Urban, G. *Sens. Actuators B* **1997**, *44*, 377−380.

(30) Harrison, D. J.; Fluri, K.; Chiem, N.; Tang, T.; Fan, Z. *Sens. Actuators B* **1996**, *33*, 105−109.

(31) Koutny, L. B.; Schmalzing, D.; Taylor, T. A.; Fuchs, M. *Anal. Chem.* **1996**, *68*, 18−22.

(32) Chiem, N.; Harrison, D. J. *Anal. Chem.* **1997**, *69*, 373−378.

(33) Duffy, D. C.; Gillis, H. L.; Goldman, J.; Sheppard, N. F.; Kellogg, G. J., unpublished results, 1999.

(34) Foulds, N. C.; Wilshere, J. M.; Green, M. J. *Anal. Chim. Acta* **1990**, *229*, 57−62.

(35) Sáchez-Cabezudo, M.; Fernández-Romero, J. M.; Luque de Castro, M. D. *Anal. Chim. Acta* **1995**, *308*, 159−163.

distribution of PNPP (diffusion coefficient, $D \approx 8 \times 10^{-6}$ cm^2/s), based on diffusion across a rectangular 100-μm-diameter channel,[17] indicated that the solutions were 90% mixed after this time, and we conclude that diffusion was effective at mixing. Longer diffusion times would, of course, be needed to achieve complete mixing in liquids more viscous than water. We note that turbulence as the liquid emptied into the read cuvette might also have helped mixing. The capillary burst valves used in the structure were designed to ensure that increases in the rate of rotation could be used to control the moment in time when the solutions were combined. Finally, the reaction mixture filled a cuvette on the edge of the disk. After this sequence had been run, the reflectance of each cuvette was measured by spinning the disk past a spectrophotometer. The reflectance measurements were then converted to absorbances for analysis. Sixty seconds was required to read the reflectance for the entire array of 48 cuvettes; the total time for fluidic processing and measurement was ~3 min.

To quantify the variation in performance between the fluidic structures, we carried out the same assay 45 times simultaneously on a disk. As with the other experiments described here, three of the read cuvettes (R4, Figure 1) were filled with solutions of known concentrations of *p*-nitrophenol to calibrate the concentration of the product of the enzyme−substrate reaction. In the remaining 45 structures, two 3-μL aliquots of 1 mg/mL alkaline phosphatase were mixed initially (instead of enzyme + inhibitor). This mixture was then combined with 6 μL of 0.5 mM PNPP, and finally the amount of product was measured. This measurement was made at a time (2 min) after which a well-mixed reaction would have reached its end point. Over 45 cuvettes, the value of $A_{430\ nm} - A_{660\ nm}$, which is proportional to the concentration of product, was 0.158 ± 0.005; i.e., the coefficient of variation in the assay was ~3.2%. Other experiments on different disks yielded similar coefficients of variation (3−3.5%). The instrument contribution to this variation, e.g., the error introduced by the optical arrangement, was 1−1.5%. The variation in the measurement introduced by the fluidic processing was, therefore, small. On occasions, runs yielded coefficients of variation of the order of 6%; these bad runs were usually due to errors by the user, e.g., loading of incorrect volumes, rather than failure of the fluidic processes on the disk.

The low variations in the absorbance measurements across a large number of cuvettes indicate that mixing of the solutions was complete, as suggested by calculation.[17] Two other pieces of evidence confirmed that mixing was complete. First, the coefficient of variation of the absorbance across a cuvette was <1%: incomplete mixing would have resulted in much greater variations in absorbance across a cuvette. Second, experiments using solutions of dye of different colors also indicated visually that mixing was complete by the time the outer cuvettes were filled with solution.

Figure 7 shows the results of 45 simultaneous enzyme + inhibitor + substrate reactions carried out on a disk. In this experiment, fixed concentrations of enzyme (0.1 mg/mL alkaline phosphatase) and substrate (5 mM PNPP), and 15 concentrations of theophylline (ranging from 0.01 to 75 mM) in triplicate, were loaded onto the disk. The disk was then run in the normal way, and the concentrations of the products were monitored by colorimetry. This experiment generated a complete isotherm for the inhibition of alkaline phosphatase by theophylline. A fit to a

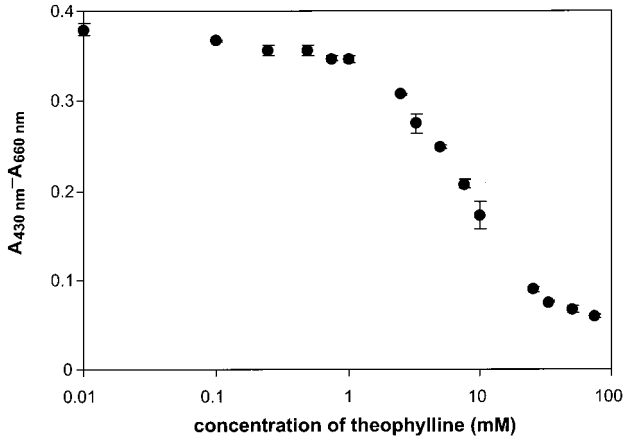

Figure 7. Forty-five enzymatic assays run simultaneously on a disk. In each case, 3 μL of 0.1 mg/mL alkaline phosphatase was mixed with 3 μL of theophylline at various concentrations. This mixture was then combined with 6 μL of 5 mM PNPP, a substrate of the enzyme. The products of the 45 enzymatic assays were monitored by measuring the absorbance at 430 nm of *p*-nitrophenol. Details of the fluidic processes are given in the text. A total of 15 concentrations of theophylline, ranging from 0.01 to 75 mM, were run in triplicate (45 assays). The results are plotted as the absorbance at 660 nm subtracted from the absorbance at 430 nm ($A_{430\ nm} - A_{660\ nm}$) as a function of the concentration of theophylline. $A_{430\ nm} - A_{660\ nm}$ is proportional to the amount of product and, hence, the activity of the enzyme. The error bars are standard deviations of the average over three measurements at each concentration. A fit of these data to the Langmuir equation yielded an inhibition constant, K_i, of (9.7 ± 0.9) mM.

Langmuir isotherm of these data yielded an inhibition constant, $K_i = (9.7 \pm 0.9)$ mM.[34] The ability to generate a complete dose−response curve for a drug in one experiment suggests applications in rapid, high-throughput screening.

Another important parameter in the biochemistry of enzymes is the Michaelis constant, K_m, that characterizes the kinetics of the reaction between an enzyme and its substrate. K_m is determined by analyzing kinetic data using the Michaelis−Menten equation:

$$v = V_{max}[S]/(K_m + [S]) \qquad (5)$$

where v is the initial rate of reaction, [S] is the concentration of substrate, and V_{max} is the maximum rate of reaction. Appropriate kinetic data are generated by measuring the initial rate of reaction over a wide range of values of [S], typically from $K_m/2$ to $8K_m$.[36]

We performed a Michaelis−Menten analysis of alkaline phosphatase in 0.1 M glycine on one disk. In this experiment, two 3-μL aliquots of 0.05 mg/mL alkaline phosphatase were loaded into 45 reservoirs usually used for enzyme and inhibitor. Aliquots (6 μL) of 15 concentrations of PNPP, ranging from 0 to 10 mM, were loaded in triplicate into the 45 reservoirs for substrate. The assays were run as described above, and $A_{430\ nm} - A_{660\ nm}$ of each cuvette was measured as a function of time. During subsequent analysis, the initial rates of reaction (v) were determined from linear fits of $A_{430\ nm} - A_{660\ nm}$ against time between 0 and 500 s.

(36) Henderson, P. J. F. In *Enzyme Assays: A Practical Approach*; Eisenthal, R., Danson, M. J., Eds.; Oxford University Press: Oxford, U.K., 1995; Chapter 10, pp 277−316.

The concentration of alkaline phosphatase (0.05 mg/mL) was chosen so that the rate of production of *p*-nitrophenol was linear over this time range. Although there is some uncertainty as to what time to take as zero for the enzyme reaction (as for any enzymatic assay), only the initial slope of $A_{430\ nm} - A_{660\ nm}$ against time ($= v$) was needed for analysis. We arbitrarily chose $t = 0$ as the time at which the solutions of enzyme and substrate mixed while the disk was being spun. A plot of v against $v/[S]$ yielded a value[36] of $K_m = (0.27 \pm 0.02) \times 10^{-3}$ M for this combination of enzyme, substrate, buffer, and temperature. This value of K_m is of the same order of magnitude as those determined for this enzyme in similar buffer systems.[37]

In these experiments, all loading of solutions onto the disk was done manually. This approach is obviously unrealistic outside a research environment or when much larger numbers of samples are involved. We believe that robotic liquid delivery systems offer a realistic solution to the problem of loading a large number of samples.[38] At their current state of development, such systems could deliver accurately small (<10 μL) volumes of liquid to a large number of reservoirs on the disk. We are also developing fluidic structures that distribute precise volumes of analytes to reservoirs by centrifugal pumping.

CONCLUSIONS

We have presented a microfluidic system based on centrifugal force that contains the central building blocks of fluidic processing, e.g., a pump, valves, and elements for mixing. When this microfluidic system is combined with methods of temperature control, detection, and information access and management that we are also developing, then we have a system capable of performing a wide range of integrated, analytical functions.

This centrifugal microfluidic system has several advantages over other microfluidic systems. First, the centrifugal pump is relatively insensitive to the chemical properties of the fluid compared to other methods. Second, the centrifugal pump is simple to implement, is safe, has low power and space requirements, and is inexpensive. Third, this pump can move fluids in a wide range of sizes of channels (we have demonstrated pumping in channels with diameters ranging from 5 to 500 μm). This property has meant that we were able to achieve a wide range of fluid pressures and flow rates (5 nL/s to 0.1 mL/s). Fourth, the configuration of the centrifugal system can often simplify detection: for example, a scanning detector is not always needed as the disk can be spun past a stationary detector. We have developed colorimetric and fluorescence detection schemes based on this principle.

A centrifugal microfluidic system also has limitations. First, a rotating system necessitates more complicated optical systems for imaging of flows, e.g., use of a stroboscope and frame buffer, or a camera attached directly to the spinning disk. Second, the direction of flow cannot be reversed. Third, this method of pumping does not have a method of chemical separation built into it, as does electrokinetic pumping. In experiments not reported here, we have, however, been able to incorporate separations on the disk by use of filters, chromatographic packing materials, and centrifugation.

Many of the benefits of this system were demonstrated by the disk containing 48 enzymatic assays. A large number of identical assays could be carried out simultaneously because a symmetric force was acting on the fluids in high-quality, identical microfluidic structures that were arranged radially on the disk. Furthermore, the flow of solutions in this assay was controlled completely passively, simply by changing the rate of rotation of the disk; no active valves were used. Finally, detection was simplified by rotating all the reaction mixtures under a fixed detector. We are also developing a disk that performs 96 simultaneous fluorescent enzymatic assays.[33] We envision applications of these disks in the life sciences and drug discovery, through genomics and proteomics, and in molecular diagnostics and genetic testing.

ACKNOWLEDGMENT

We thank our colleagues at Gamera Bioscience, especially Bruce L. Carvalho and Jeff Goldman, for helpful discussions and experimental assistance during the course of this work. We thank Prof. Marc Madou (Ohio State University) for helpful discussions. We are grateful to Rebecca J. Jackman for help with profilometry.

Received for review June 21, 1999. Accepted August 10, 1999.

AC990682C

(37) Foulds, N. C.; Frew, J. E.; Green, M. J. In *Biosensors: A Practical Approach*; Cass, A. E. G., Ed.; Oxford University Press: Oxford, U.K., 1990; Chapter 4, pp 97−124.

(38) Persidis, A. *Nature Biotechol.* **1998**, *16*, 488−489.